DMD Fast Forward. Published on August 23, 2007 as doi:10.1124/dmd.107.017343

DMD #17343

Title Page

Analysis of CYP2A Contributions to Metabolism of 4-(Methylnitrosamino)-1-(3-pyridyl)-1-butanone (NNK) in Human Peripheral Lung Microsomes

Pamela J. Brown, Leanne L. Bedard, Ken R. Reid, Dimitri Petsikas, and Thomas E. Massey

Departments of Pharmacology and Toxicology (P.B., L.B., T.M.) and Surgery (K.R., D.P.), Queen's University, Kingston, Ontario, Canada, K7L 3N6

Running Title Page

Running Title: CYP2A and human lung microsomal NNK metabolism.

To whom correspondence should be addressed:
Dr. Thomas E. Massey
Professor and Head
Department of Pharmacology and Toxicology
Queen's University
Kingston, ON K7L 3N6
Canada
Phone: (613) 533-6115
Fax: (613) 533-6412
E-mail. masseyt@queensu.ca

Number of text pages: 23

Number of tables: 3

Number of figures: 5

Number of references: 34

Number of words:
Abstract - 239
Introduction - 691
Discussion - 1602

Abbreviations: NNK, 4-(methylnitrosamino)-1-(3-pyridyl)-1-butanone; NNAL, 4-(methylnitrosamino)-1-(3-pyridyl)-1-butanol; NNK-*N*-oxide, 4-(methylnitrosamino)-1-(3-pyridyl *N*-oxide)-1-butanone; NNAL-*N*-oxide, 4-(methylnitrosamino)-1-(3-pyridyl *N*-oxide)-1-butanol; keto alcohol, 4-hydroxy-1-(3-pyridyl)-1-butanone; diol, 1-(3-pyridyl)-1,4-butane diol; keto acid, 1-(3-pyridyl)-1-butanone-4-carboxylic acid; hydroxy acid, 1-(3-pyridyl)-1-butanol-4-carboxylic acid; CYP, cytochrome P450; HPLC, high performance liquid chromatography; TSNAs; tobacco specific nitrosamines; GAPDH, glyceraldehyde-3-phosphate dehydrogenase.

Abstract

The objectives of this study were to determine the contributions of CYP2A13 and CYP2A6 to 4-(methylnitrosamino)-1-(3-pyridyl)-1-butanone (NNK) metabolism in human peripheral lung microsomes and to determine the influence of the genetic polymorphism, CYP2A13 Arg257Cys on NNK metabolism. NNAL, the keto-reduced metabolite of NNK, was the major metabolite produced, ranging from 0.28 to 0.9 %/mg protein/min. Based on total bioactivation of NNK and NNAL by α-carbon hydroxylation, subjects could be classified as either high (17 subjects) or low (12 subjects) bioactivators ($(5.26 \pm 1.23)x10^{-2}$ and $(6.49 \pm 5.90)x10^{-3}$ % total α-hydroxylation/mg protein/min, $P< 0.05$). Similarly, for detoxification, subjects could be grouped into high (9 subjects) and low (20 subjects) categories ($(2.03 \pm 1.65)x10^{-3}$ and $(2.50 \pm 3.04)x10^{-4}$ % total *N*-oxidation/mg protein/min, $P<0.05$). When examining data from all individuals, no significant correlations were found between levels of CYP2A mRNA, CYP2A enzyme activity or CYP2A immunoinhibition and the degree of total NNK bioactivation or detoxification ($P>0.05$). However, subgroups of individuals were identified for whom CYP2A13 mRNA correlated with total NNK and NNAL α-hydroxylation and NNAL-*N*-oxide formation ($P <0.05$). The degree of NNAL formation and CYP2A13 mRNA were also correlated ($P<0.05$). Subjects (n=84) were genotyped for the CYP2A13 Arg257Cys polymorphism, and NNK metabolism for the one variant (Arg/Cys) was similar to that for other subjects. Although results do not support CYP2A13 or CYP2A6 as predominant contributors to NNK bioactivation and detoxification in peripheral lung of all individuals, CYP2A13 may be important in some.

Lung cancer is the leading cause of cancer-related death in the world and it is estimated that cigarette smoking accounts for approximately 90% of lung cancer cases (Hecht, 2003). The tobacco-specific nitrosamine (TSNA) 4-(methylnitrosamino)-1-(3-pyridyl)-1-butanone (NNK) is thought to play a major role in human tobacco-related cancers (Hecht, 2003). NNK is the most prevalent pulmonary carcinogen in tobacco smoke and the most potent cancer-causing TSNA in all animal species tested (Hecht, 1998). NNK selectively induces lung adenocarcinoma in animals (Hecht, 1998) and is believed to be a causal agent in the induction of human lung adenocarcinoma, which is now the leading form of lung cancer (Thun et al., 1997 ; Hoffmann et al., 1996).

To induce carcinogenesis, NNK and its keto-reduced metabolite, 4-(methylnitrosamino)-1-(3-pyridyl)-1-butanol (NNAL) require metabolic activation via α-carbon hydroxylation (Figure 1). Hydroxylation of the α-methylene carbons of NNK and NNAL leads to the formation of DNA methylating species, while hydroxylation of the α-methyl carbons of NNK and NNAL results in the formation of DNA pyridyloxobutylating and pyridylhydroxybutylating species, respectively. The formation of both types of adducts is believed to be important in the induction of carcinogenicity by NNK since less potent nitrosamines will only either methylate or alkylate DNA (Hecht, 1999). α-Carbon hydroxylation of NNK and NNAL also results in the formation of four endpoint metabolites, keto acid, keto alcohol, hydroxy acid and diol. These endpoint metabolites are used in assessing the degree of NNK bioactivation, since their formation is indicative of the formation of the DNA-reactive metabolites. The detoxification of NNK and NNAL occurs mainly through pyridine *N*-oxidation, which results in the formation of excretable *N*-oxides (Hecht, 1998).

Cytochromes P450 (CYPs), specifically CYP2A6/2A13, CYP2B6, CYP3A4/3A5 and CYP2E1 (Smith et al., 1992 ; Smith et al., 1995 ; Hecht, 1998 ; Smith et al., 1999 ; Smith et al., 2003), and prostaglandin H synthase (Smith et al., 1995 ; Smith et al., 1999 ; Smith et al., 2003) but not lipoxygenases (Bedard et al., 2002) have been implicated in human pulmonary NNK metabolism. Of particular interest are the CYP2A isozymes CYP2A13 and CYP2A6. CYP2A13 is expressed predominantly in the human respiratory tract including the nasal mucosa, trachea and peripheral lung (Su et al., 2000), and heterologously-expressed CYP2A13 exhibits higher catalytic activity for NNK activation than do other CYP isoforms examined (Su et al., 2000 ; Smith et al., 1992 ; Patten et al., 1996). A functional polymorphism resulting from a C/T transition in exon 5 of the *CYP2A13* gene that leads to an Arg/Cys amino acid substitution at residue 257, significantly reduces the enzyme's activity towards several different substrates, including NNK (Zhang et al., 2002). A potential protective effect against NNK-induced carcinogenesis for individuals possessing this variant allele is supported by an epidemiological study which found that individuals with variant CYP2A13 genotype (CT and TT) had a reduced risk of lung adenocarcinoma compared to individuals with wildtype (CC) genotype (Wang et al., 2003). The other CYP2A isozyme, CYP2A6, is the main CYP2A isoform in liver (Su et al., 2000) but is also present in human nasal mucosa, trachea and lung (Su et al., 2000). CYP2A6 is a major catalyst of nicotine and coumarin metabolism (Messina et al., 1997 ; Fernandez-Salguero and Gonzalez, 1995) and is thought to be one of the major CYP isoforms responsible for NNK activation (Yamazaki et al., 1992 ; Smith et al., 2003). The role of CYP2A6 in lung cancer is not clear as studies that have examined the relationship between CYP2A6 polymorphisms

and lung cancer risk have been conflicting. In one study CYP2A6 deficiency has been correlated with reduced lung cancer risk (Miyamoto et al., 1999) while another study showed no relationship (Wang et al., 2003).

Because of their established involvement in NNK bioactivation and their expression in human lung, it can be suggested that CYP2A13 and CYP2A6 may contribute largely to human pulmonary NNK metabolism.

In the present study, lung tissue from a relatively large sample size of individuals (n=29) was used to assess NNK biotransformation among individuals, and specifically the importance of both CYP2A13 and CYP2A6 in these pathways. In addition, the influence of the CYP2A13 Arg257Cys genetic polymorphism on NNK metabolism was assessed.

Methods

Chemicals. Chemicals were obtained as follows: [5-^{3}H]NNK (2.4-11.0 Ci/mmol; >98% pure) from Chemsyn Science Laboratories (Lenexa, KS) and Moravek Biochemicals (Brea, CA); NNK, NNAL, 4-(methylnitrosamino)-1-(3-pyridyl-N-oxide)-1-butanone (NNK-*N*-oxide), 4-(methylnitrosamino)-1-(3-pyridyl-N-oxide)-1-butanol (NNAL-*N*-oxide), 4-hydroxy-1-(3-pyridyl)-1-butanone (keto alcohol), 1-(3-pyridyl)-1,4-butane diol (diol), 1-(3-pyridyl)-1-butanone-4-carboxylic acid (keto acid), 1-(3-pyridyl)-1-butanol-4-carboxylic acid (hydroxy acid), from Toronto Research Chemicals (North York, ON); Uniscint BD radioflow scintillation cocktail from National Diagnostics (Atlanta, GA); glucose-6-phosphate dehydrogenase, coumarin, 7-hydroxycoumarin and 7-hydroxy-4-methylcoumarin from Sigma-Aldrich Co. (St. Louis, MO). All other chemicals were reagent grade and were obtained from common commercial suppliers.

Tissue Procurement. Sections of peripheral human lung tissue devoid of visible tumors were obtained from patients undergoing clinically indicated lobectomy at Kingston General Hospital. Tissue specimens were cut into 1.5-cm^{3} pieces, wrapped in aluminum foil, frozen in liquid N_2, and stored at -80°C until microsome preparation (Smith et al., 2003). Histological analysis was performed on tissues to confirm the absence of microscopic tumors. Data regarding surgical diagnosis, gender, smoking history, potential occupational carcinogen exposure and drug treatments for the month prior to surgery were collected to identify possible confounders including the possible inductive/inhibitory effects of certain drug treatments on biotransformation enzymes. Patients were classified as former smokers if smoking termination was reported to be >2 months before surgery (McLemore et al., 1990).

Preparation of Human Lung Microsomes. Human whole peripheral lung microsomes were prepared as described (Smith et al., 2003). Briefly, tissue specimens were thawed on ice for 15 min. They were then rinsed, chopped, and homogenized in 0.1 M potassium phosphate buffer containing 1.15 % KCl (pH 7.4) using a Polytron homogenizer, and microsomes were prepared by differential centrifugation (Donnelly et al., 1996). Protein concentration was determined by the method of Lowry *et al.*, (1951) using bovine serum albumin as a standard.

Incubations with NNK. Before use, the purity of [5-^{3}H]NNK was assessed, since high purity (>98%) was needed to ensure that impurities would not interfere with quantification of metabolites. If purity was <98%, [5-^{3}H]NNK was purified by HPLC as described (Smith et al., 1999). Incubation mixtures were prepared as described (Smith et al., 2003), using 4.2 μM [5-^{3}H]NNK and 1.0 mg microsomal protein in a total volume of 1.0 ml. In addition to samples that contained the complete incubation mixture, samples without the NADPH-generating system and samples bubbled with carbon monoxide (CO) were also prepared to assess the overall contribution of P450s. All metabolite analyses were performed in duplicate. NNK metabolite formation by human lung microsomes has been demonstrated to be linear for at least 30 min (Smith et al., 2003).

Assessment of NNK Biotransformation. NNK metabolites were quantified by reverse-phase gradient HPLC with radiometric detection (Smith et al., 2003). For immunoinhibition, 1.0 mg of microsomal protein and 200 μg of anti-CYP2A6/13 (BD Gentest, Woburn, MA) were incubated on ice for 20 min prior to use in incubations, as recommended by the supplier. For each metabolite, the amount produced was expressed as a percentage of the total radioactivity recovered from [5-^{3}H]NNK plus metabolites per

milligram of protein per minute, to account for differences in recovery of [5-^{3}H]NNK between incubates. Metabolite peaks were quantified only if they were at least twice background radioactivity levels.

CYP2A mRNA Expression. Total RNA was isolated from human lung tissue (n=28) using the Qiagen RNeasy Mini Kit, with an additional on-column DNase treatment step in accordance with the manufacturer's instructions (Qiagen, Valencia, CA). The quality of the RNA samples was determined by electrophoretic analysis of 3 µg of RNA on a denaturing gel. Ethidium bromide staining of the gel detected distinct 28S and 18S rRNA bands with an intensity ratio of 28S:18S of at least 1.5. The UV absorbance ratio (260 nm/280 nm) ranged from 1.8 to 2.1 for all RNA samples. cDNA was synthesized from 5µg of total RNA in a reaction volume of 50 µl using the High Capacity cDNA Archive Kit (Applied Biosystems, Foster City, CA). For quantitative real-time PCR, 2µl aliquots of cDNA were amplified using CYP2A13 and CYP2A6 TaqMan primer and probes sets (Applied Biosystems, Foster City, CA; Assay ID Hs00426372_m1 and Hs00868409_s1, respectively) according to the manufacturer's recommendations. Amplification, detection and analysis were performed using Smart Cycler II instrumentation and software (Cepheid, Sunnyvale, CA). CYP2A13 and CYP2A6 gene expression was normalized using GAPDH as an endogenous reference. For mRNA quantitiation, the comparative C_T method was used since the relative PCR efficiencies for target and reference amplification were approximately equal. PCR product specificity was verified by the presence of a single PCR product after performing agarose gel electrophoresis with ethidium bromide staining. Due to limitations in tissue availability both CYP2A13 and CYP2A6 gene expression could not be assessed for all individuals.

Coumarin 7-Hydroxylase Activity. Currently, there are no CYP2A13 or CYP2A6 isozyme-specific substrates available. Since CYP2A13 and CYP2A6 both metabolize coumarin at the 7-position, coumarin 7-hydroxylation is often used as a probe activity for the CYP2A enzymes (von Weymarn et al., 2005). 7-Hydroxycoumarin formation was assessed in isolated human lung microsomes (n=28) and in human CYP2A6 microsomes (BD Biosciences, Woburn, MA) as a positive control, according to the manufacturer's protocol, but with some modifications. Reaction mixtures containing 0.2 mM coumarin in a 250 µl total reaction volume were pre-incubated at 37°C for 5 min and then incubated for an additional 25 min after addition of 0.3 mg of microsomal protein. Levels of 7-hydroxycoumarin and the internal standard, 7-hydroxy-4-methylcoumarin were assessed using a Shimadzu chromatographic system (Mandel Scientific, Guelph, ON) with RF-10Axl fluorescence detector and CLASS-VP (v. 7.2.1 SP1) software as described (www.cypex.co.uk/) with some modifications. The mobile phase consisted of 75/25 (v/v) 0.05% orthophosphoric acid/acetonitrile, delivered isocratically at 1.0 ml/min through a Supelcosil 5 micron LC-18 (15 cm by 4.6 mm) column (Sigma-Aldrich, St. Louis, MO) at room temperature. Fluorescence was determined with excitation at 324 nm and emission at 458 nm. Levels of 7-hydroxycoumarin formation were quantified by subtracting the fluorescence of boiled microsome samples and comparing to a standard curve of 7-hydroxycoumarin to 7-hydroxy-4-methylcoumarin peak area ratios as a function of 7-hydroxycoumarin concentration. 7-hydroxycoumarin formation was linear up to 1 mg of microsomal protein and for 30 min.

Polymorphism Analysis. Genomic DNA was isolated from peripheral lung tissue by protease digestion followed by standard phenol:chloroform extraction and ethanol precipitation (Devereux et al., 1993). Genotypes (n=84) for CYP2A13 at the C3375T (Arg257Cys) site were assessed by PCR-RFLP analysis (Wang et al., 2003) with some modifications. Reaction conditions were as follows: 15 min at 95°C, 13 cycles of 30 s at 94°C, 30 s at 63°C (step-down 0.5°C/cycle) and 50 s at 72°C, followed by 20 cycles of 30 s at 94°C, 30 s at 57.5°C and 50 s at 72°C and a final elongation step of 5 min at 72°C. The PCR reaction resulted in a 375-bp product. Ten µl of PCR product were digested with 2.9 units of *Hha*I (New England Biolabs, Inc., Beverly, MA) and restriction products were separated on a 3% agarose gel. The wild-type C allele had a *Hha*I restriction site that resulted in two bands (217 and 158 bp) and the variant T allele resulted in the elimination of the restriction site, producing a single 375-bp band.

Statistical Analysis. For microsomal NNK biotransformation, individual metabolite values represent the mean of duplicate incubations. When grouped, microsomal data are presented as means ± standard deviations (SD). Statistically significant differences in grouped microsomal data were determined by a Student's *t* test and a Student's *t* test with Welch's correction if heterogeneity of variance was present. All correlation analyses were performed using Pearson Product Moment correlation analysis (GraphPad Prism 4 Software). $P<0.05$ was considered statistically significant in all cases. To determine if NNK bioactivation and detoxification group data were normally distributed, an Anderson-Darling Normality test was used. Group data with $P<0.05$ were considered to have a non-normal distribution.

Results

Patient Demographics. Microsomes were prepared from sections of peripheral lung obtained from 30 human subjects (17 males and 13 females) from eastern Ontario, aged 62.6 ± 10.5 years (Table 1). Due to limitations in tissue availability, microsomes from all 30 subjects could not be used in all analyses. Based on reported smoking histories, 16 individuals were current smokers, 12 were former smokers and information for two individuals was not available.

NNK Biotransformation in Lung Microsomes. NNAL was the major metabolite produced from NNK, with formation ranging from 0.280 to 0.900%/mg protein/min (representing ~ 8 to 27 pmol NNAL/mg protein/min). Total bioactivation, represented by the sum of the four α-carbon hydroxylation endpoint metabolites, ranged from $< 3.33 \times 10^{-4}$ to 7.50×10^{-2} % total α-hydroxylation/mg protein/min (representing ~ 0.01 to 2.3 pmol α-hydroxylation/mg protein/min). Total *N*-oxidation, represented by the sum of the two *N*-oxides, ranged from $< 3.33 \times 10^{-4}$ to 1.33×10^{-3} % total *N*-oxidation/mg protein/min (representing ~ 0.01 to 0.04 pmol *N*-oxidation/mg protein/min). In all metabolism analyses, individuals with metabolism below the lower limit of detection were assigned a value of 0 % total metabolism/mg protein/min. Normality tests of bioactivation and detoxification group data revealed that each group was not normally distributed ($P<0.05$). Subsequently, based on total bioactivation, subjects could be classified as either high (17 subjects) or low (12 subjects) bioactivators, with significantly different mean total α-hydroxylation activities ($(5.26 \pm 1.23) \times 10^{-2}$ and $(6.49 \pm 5.90) \times 10^{-3}$ % total α-hydroxylation/mg protein/min, respectively, n=29, $P< 0.05$) (Figure 2a). Similarly, based on total detoxification, subjects could be grouped into high (9 subjects)

and low (20 subjects) categories, with significantly different mean total *N*-oxidation activities ($(2.03 \pm 1.65)x10^{-3}$ and $(2.50 \pm 3.04)x10^{-4}$ % total *N*-oxidation/mg protein/min, respectively, n=29, $P<0.05$) (Figure 2b). No correlation between NNK bioactivation and detoxification activities for individuals was found ($P>0.05$). Also, no correlation was found between the degree of NNK bioactivation or detoxification and patients' age, gender or smoking status ($P>0.05$). Smoking status was compared among high and low bioactivation groups and it was found that 71% of high bioactivators and 36% of low bioactivators were current smokers. Potential effects of drug treatments on NNK metabolism were assessed and no observable differences were found in the NNK metabolite profiles of individuals taking drugs that may alter the activities of relevant CYPs, as compared to those of other subjects. NNAL formation was not significantly different between the high and the low bioactivation or detoxification groups ($P>0.05$).

Formation of the NNK-derived α-hydroxylation metabolites keto acid and keto alcohol was significantly higher than formation of the NNAL-derived hydroxy acid and diol, in both the high and low bioactivation groups ($P<0.05$) (Table 2). When comparing metabolite formation between groups, production of hydroxy acid, keto acid and keto alcohol was significantly higher (~4 times, ~6 times and ~26 times, respectively) in the high compared to the low bioactivation group, while formation of diol, which was highly variable between individuals, was not significantly different between groups ($P>0.05$). Formation of total NNK-derived metabolites (i.e. keto acid plus keto alcohol) but not total NNAL-derived metabolites (i.e. hydroxyl acid plus diol) was significantly different between the high and low bioactivaton groups ($P<0.05$).

Removal of the NADPH-generating system decreased total α-hydroxylation in tissues from the majority of subjects, by 3.6 to 100 % (median decrease =79.6%, n=21), but had increased or no apparent effect in microsomes from three subjects. Treatment with CO decreased total α-hydroxylation by 54.4 to 100 % (median decrease =66.7%) in microsomes from nine subjects and increased bioactivation by 2.12 to 140 % (median increase =34%) in microsomes from 13. Similarly, removal of the NADPH generating system decreased total *N*-oxidation by 25.0 to 100 % (median decrease =100%) in 13 subjects' microsomes, increased *N*-oxidation by 13.3 to 66.7 % (median increase =59.9%) in three, and had no effect in eight. CO decreased total *N*-oxidation by 25.1 to 100 % (median decrease =100%) in 14 subjects' microsomes, increased *N*-oxidation by 1.01 to 300 % (median increase =41.7%) in six, and had no apparent effect on NNK and NNAL *N*-oxidation in microsomes from four subjects. CO treatment eliminated NNAL formation in microsomes from two subjects and increased it by 3.77 to 329 % (median increase =165%) in 22 subjects. In contrast, removal of the NADPH-generating system completely eliminated NNAL formation in microsomes from all subjects (n=24).

CYP2A13 mRNA Expression and NNK Biotransformation. Regardless of whether high and low bioactivators and detoxifiers were considered separately or pooled, there was no significant correlation between CYP2A13 mRNA levels and the degree of total NNK bioactivation (Figure 2a) or detoxification (Figure 2b). Also, no significant associations were found between CYP2A13 mRNA levels and formation of individual α-hydroxylation metabolites. However, examination of the CYP2A13 mRNA and total α-hydroxylation scatter plot revealed the existence of a subgroup (n=4) with both high levels of CYP2A13 mRNA and a high degree of total α-hydroxylation, for whom

DMD Fast Forward. Published on August 23, 2007 as DOI: 10.1124/dmd.107.017343
This article has not been copyedited and formatted. The final version may differ from this version.

CYP2A13 levels positively correlated with the degree of NNK bioactivation (r=0.967, $P<0.05$). Analysis of the two *N*-oxides (detoxification products) independently revealed no significant correlations between CYP2A13 mRNA expression and levels of NNAL-*N*-oxide (r=0.294, $P>0.05$) or NNK-*N*-oxide (r=-0.022, $P>0.05$). However, when subjects that had no detectable NNAL-*N*-oxide formation were excluded, a significant association was found between CYP2A13 mRNA expression and levels of NNAL-*N*-oxide (n=5, r=0.925, $P<0.05$). Of these five individuals, three were high bioactivators. A statistically significant correlation occurred between the extent of NNAL formation and CYP2A13 mRNA expression ($P<0.05$) (Figure 2c). However, when individuals (n=3) with relatively high levels of CYP2A13 mRNA and high levels of NNAL formation were excluded from the analysis, this correlation was no longer significant (r=-0.0658, $P>0.05$).

CYP2A6 mRNA Expression and NNK Biotransformation. When high and low bioactivators and detoxifiers were considered separately or pooled, there was no significant correlation between CYP2A6 mRNA levels and the degree of total NNK bioactivation (Figure 3a), detoxification (Figure 3b) or NNAL formation (Figure 3c). Similarly, no correlation was found between levels of CYP2A13 and CYP2A6 mRNA among individuals (n=24, r=0.114, $P>0.05$).

Coumarin 7-Hydroxylase Activity and NNK Biotransformation. Regardless of whether high and low bioactivators and detoxifiers were considered separately or pooled, there was no significant correlation between coumarin 7-hydroxylation and the degree of total NNK bioactivation (Figure 4a) or detoxification (Figure 4b). 7-Hydroxycoumarin formation correlated with formation of hydroxy acid (r=0.512,

P<0.05) but not with other individual α-hydroxylation metabolites. Correlation analysis between the degree of NNK bioactivation and coumarin 7-hydroxylation for the high bioactivation subgroup could not be carried out because of limited tissue availability for two subjects. There was no association between NNAL formation and 7-hydroxycoumarin formation (*P*>0.05). However, when individuals with relatively high levels of 7-hydroxycoumarin formation (>20 fmol/mg protein/min, n=2) were excluded from analyses, a significant correlation was found (r=0.520, *P*<0.05) (Figure 4c). There was no difference in mean coumarin 7-hydroxylation activity between current and former smokers (7.25± 14.5 fmol/mg protein/min (95% CI: -0.488 to 15.00 fmol.mg protein/min) and 8.55±7.02 fmol/mg protein/min (95% CI: 3.84 to 13.3 fmol/mg protein/min), respectively). However, there was a positive relationship between age and coumarin 7-hydroxylation activity among individuals (n=27, r=0.387, *P*<0.05) and males had significantly higher activity than did females (11.6±15.0 fmol/mg protein/min, n=15 (95% CI: 3.25 to 19.9 fmol/mg protein/min) and 3.07±2.00 fmol/mg protein/min, n=12 (95% CI: 1.80 to 4.33 fmol/mg protein/min), respectively, *P*<0.05).

To determine the consistency between enzymatic activity as reflected by coumarin hydroxylation and CYP2A expression as assessed by mRNA levels, correlation analysis was performed. When results from all individuals were pooled, no significant correlations were found between 7-hydroxycoumarin formation and either CYP2A13 mRNA levels (n=26, r=-0.0685, *P*>0.05) or CYP2A6 mRNA levels (n=22, r=-0.354, *P*>0.05) (Figure 5).

Immunoinhibition of NNK Biotransformation. The presence of the CYP2A6/13 inhibitory antibody decreased total α-hydroxylation by 0.35 to 98.3 %

(median decrease =10.1%) in 16 subjects' microsomes, increased it by 1.52 to 57.5 % (median increase =5.42%) in eight and had no apparent effect in microsomes from six subjects. It decreased total *N*-oxidation by 22.2 to 100 % (median decrease =85.0%) in 14 subjects' microsomes, increased *N*-oxidation by 25.3 and 200 % in two, and had no effect in 14. NNAL formation was decreased by 1.00 to 38.8 % (median decrease =8.10%) in microsomes from 19 subjects and increased by 4.33 to 50.5 % (median increase =14.6%) in ten. Regardless of whether high and low bioactivators and detoxifiers were considered separately or together, there was no significant correlation between the % change in NNK bioactivation or detoxification in the presence of a CYP2A6/13 inhibitory antibody and either the degree of NNK metabolism formation of individual α-hydroxylation or *N*-oxidation metabolites (Table 3). There also was no significant correlation between NNAL formation and the % change in NNAL formation in the presence of a CYP2A6/13 inhibitory antibody (Table 3).

When assessing the consistency between CYP2A immunoinhibition-mediated changes in NNK metabolism and the measures of assessing CYP2A expression or activity, no significant correlations were found between levels of CYP2A13 or CYP2A6 mRNA and CYP2A6/13 immunoinhibition-mediated changes in total NNK bioactivation, total NNK detoxification, or NNAL formation. Similarly, no significant correlations were found between 7-hydroxycoumarin formation and CYP2A6/13 immunoinhibition-mediated changes in total NNK bioactivation, total NNK detoxification, or NNAL formation (Table 3).

Effects of CYP2A13 Arg257Cys polymorphism on NNK biotransformation. Following PCR-RFLP analysis, homozygous wildtype (C/C) samples produced the

anticipated products of 217 bp and 158 bp (Wang et al., 2003), whereas heterozygous variant (C/T) samples produced products of 375 bp, 217 bp and 158 bp. The resultant genotype frequencies were 83/84 (98.8 %) C/C, 1/84 (1.2 %) C/T and 0/84 (0%) T/T. NNK metabolite profile for the one heterozygous variant (0.047 % total α-hydroxylation/mg protein/min; 0.00133 % total *N*-oxidation/mg protein/min; 0.316 % NNAL formation/mg protein/min) did not differ from those of the C/C subjects.

Discussion

Although we have previously used inhibitors to assess CYP2A6 contributions to NNK metabolism in adult human lung (Smith et al., 2003), this is the first study to assess CYP2A13 contributions. Examination of CYP2A13-mediated NNK metabolism was of interest as this human CYP is expressed predominantly in the lung (Su et al., 2000) and is the most catalytically active CYP isoform in the metabolic activation of NNK (Su et al., 2000). Our grouped results suggest no correlation between the degree of NNK bioactivation or detoxification and CYP2A gene expression and activity. However, a subgroup of individuals was identified for whom high levels of NNK bioactivation correlated with high CYP2A13 mRNA levels (Figure 2a), suggesting that CYP2A13 may contribute substantially to NNK bioactivation in some, but not all individuals. Similarly, for NNK detoxification, a subgroup of individuals was identified for whom CYP2A13 mRNA expression correlated with detectable levels of NNAL-*N*-oxide. However, the pooled results suggest that CYP2A13 is not the sole enzyme contributing to NNK metabolism in peripheral human lung microsomes. The apparent discrepancy between our results and those reported for fetal nasal microsomes (Wong et al., 2005) may reflect the fact that levels of CYP2A13 mRNA (Su et al., 2000) and CYP2A13 immuno-reactive protein (Zhu et al., 2006) are considerably higher in the nasal mucosa than in the lung. Hence, in areas of the respiratory system where CYP2A13 levels are lower, other enzymes may contribute substantially to NNK metabolism.

Based on the interindividual variability in NNK metabolism, individuals were classified into high or low bioactivation and detoxification groups. The observation of distinct groups is consistent with our previous study of seven subjects (Smith et al.,

2003). The distribution of subjects between bioactivation categories is not consistent with reported frequencies of established genetic polymorphisms of enzymes that have been characterized with respect to NNK metabolism, suggesting the possibility that environmental factors, rather than genetics, make the largest contribution to interindividual variability in NNK metabolism.

Although the levels of total NNK-derived metabolites were markedly different between the high and low bioactivation groups, the levels of total NNAL-derived metabolites were not significantly different (Table 2). This was unexpected because it was anticipated that the NNAL-derived metabolites would vary between the groups to the same extent as the NNK-derived metabolites, since both the high and low bioactivation groups formed equal amounts of NNAL. The differences in NNK and NNAL metabolism may be due to differences in the affinity of different CYP isoforms for NNK versus NNAL as a result of differences in polarity between the keto group of NNK and the hydroxyl group of NNAL. In fact, Jalas *et al.* (2003) found that CYP2A enzymes are more efficient catalysts of NNK metabolism than of NNAL metabolism.

CYP involvement in human pulmonary microsomal NNK metabolism was supported by NADPH-dependence but as consistent with previous studies (Smith et al., 1992 ; Smith et al., 1995) sensitivity to CO inhibition was variable. The fact that removal of the NAPDH-generating system and CO treatment did not completely inhibit NNK metabolism in some individuals suggests that non CYP enzymes may also be involved in the metabolism.

Consistent with previous results (Smith et al., 2003 ; Maser et al., 2000), NNAL formation from NNK was NADPH-dependent for all subjects, but our results are the first

to suggest a role for CYP2A13 in catalyzing the carbonyl reduction of NNK to form NNAL. This role is supported by our finding that NNAL formation positively correlated with CYP2A13 mRNA levels, although this correlation was dependent upon inclusion of individuals with high levels of CYP2A13 mRNA. It is also supported by the observation that NNAL formation positively correlated with the degree of 7-hydroxycoumarin formation in all individuals with the exception of those with relatively high coumarin 7-hydroxylation activity. It is possible that coumarin 7-hydroxylation is mainly CYP2A6-mediated in individuals with relatively high levels 7-hydroxycoumarin formation. It has been suggested that the microsomal enzyme, 11β-hydroxysteroid dehydrogenase (11β-HSD) rather than P450s, is the major catalyst of this reaction (Hecht, 1998). However, in microsomes from human lung, NNAL formation was insensitive to an 11β-HSB inhibitor (Breyer-Pfaff et al., 2004) and sensitive to P450 inhibitors. In contrast to results from the present study, an anti-CYP2A antibody did not inhibit NNAL formation in human fetal nasal microsomes (Wong et al., 2005). However, since fetal tissues had been pooled, interindividual variability in CYP2A13 contributions to NNAL formation could not be assessed. As well, age is known to affect P450 activity (Day et al., 2006).

Results presented here are also the first to support involvement of CYP2A13 in NNAL detoxification in human lung tissue for some individuals. While no significant correlations were found between CYP2A13 mRNA and either total NNK detoxification or NNK-*N*-oxide levels, an association was found between levels of NNAL-*N*-oxide and CYP2A13 mRNA. This result is consistent with the finding that heterologously-expressed CYP2A13 is capable of catalyzing NNAL *N*-oxidation but not NNK *N*-oxidation (Jalas et al., 2003).

No correlations were found between the degree of total NNK bioactivation or detoxification and 7-hydroxycoumarin formation, the latter of which is expected to reflect overall CYP2A activity. However, assessing associations between CYP2A13 or CYP2A6 activity and NNK metabolism is difficult since available substrates with the exception of the drug phenacetin, do not discriminate between CYP2A13 and CYP2A6, and because CYP2A6 is 10 times more active than CYP2A13 at catalyzing coumarin 7-hydroxylation (Su et al., 2000). While recently it was shown that CYP2A13 can efficiently metabolize phenacetin and CYP2A6 has virtually no catalytic activity towards this drug (Fukami et al., 2007), phenacetin is also a CYP1A2 substrate. Since CYP1A2 can also potentially bioactivate NNK (Smith et al., 1996) and is expressed in human lung (Wei et al., 2001),using phenacetin to assess CYP2A13 activity in human lung microsomes would also be problematic. When examining associations between individual α-hydroxylation metabolites and 7-hydroxycoumarin formation, a significant correlation was found between the degree of hydroxy acid formation and 7-hydroxycoumarin. This finding is consistent with both CYP2A13 and CYP2A6 being more efficient catalysts of α-methylene hydroxylation compared to α-methyl hydroxylation (Su et al., 2000 ; Jalas et al., 2003). Since neither CYP2A13 nor CYP2A6 mRNA correlated with hydroxy acid formation, the relative contribution of these isoforms is not known.

The absence of significant correlations between the degree of NNK bioactivation, detoxification or keto reduction and CYP2A immunoinhibition may also reflect the fact that specific contributions of either CYP2A13 or CYP2A6 to NNK metabolism are difficult to assess since commercially available inhibitory antibodies do not discriminate

between CYP2A13 and CYP2A6 (Su et al., 2000). Moreover, an attempt was made to determine the relative CYP2A protein levels among individuals by immunoblotting; however protein levels were too low for detection. While our results do not suggest uniform involvement of CYP2A13 in NNK metabolism across all individuals, the possibility exists that more specific measures of enzyme contributions would reveal that a correlation exists for a greater proportion of individuals.

In some microsomal samples, the presence of the CYP2A6/13 inhibitory antibody increased levels of NNK metabolism. It has been suggested that non-uniform constitution of human microsomes between incubates and cigarette smoke particulate matter might affect how NNK biotransformation activities are expressed in different incubates (Smith et al., 2003).

No statistically significant correlations were found between CYP2A13 or CYP2A6 mRNA levels and 7-hydroxycoumarin formation when tissues from all patients were considered (Figure 4 and 5). The lack of associations may be due to the fact that 7-hydroxycoumarin formation is a measure of overall CYP2A enzyme activity, not specifically CYP2A13 or CYP2A6 (Su et al., 2000). In addition, nicotine is a mechanism-based inactivator of both CYP2A13 and CYP2A6 (von Weymarn et al., 2006), so current smokers could potentially have had diminished CYP2A enzyme activity. However, a higher proportion of current smokers were actually high bioactivators as compared to low bioactivators and levels of 7-hydroxycoumarin formation did not differ between current and former smokers. There also were no significant correlations between the CYP2A immunoinhibition of NNK metabolism and CYP2A13 mRNA levels or CYP2A6 mRNA levels or 7-hydroxycoumarin formation

(Table 3). Inconsistency between these parameters could be attributed to a lack of specificity of the antibody for either CYP2A isoform (e.g. according to information from the supplier, the antibody reacts with CYP2A6, CYP2A13 and mildly with CYP2E1).

Genotype frequencies for the CYP2A13 Arg257Cys polymorphism were consistent with those previously published for a Caucasian population (96.2% (C/C), 3.8% (C/T) and 0% (T/T) (Zhang et al., 2002). While NNK metabolism for the one heterozygous variant did not differ from other subjects, it is not possible to accurately determine the actual contribution of this polymorphism to NNK metabolism, since only one variant was found. The current study did not assess the influence of CYP2A6 polymorphisms on NNK metabolism since no clear associations have been found between CYP2A6 polymorphisms and lung cancer risk (Wang et al., 2003 ; Raunio et al., 2001).

In summary, examination of the interindividual differences in the pulmonary microsomal metabolism of NNK revealed the existence of high and low bioactivation and detoxification groups. Differences in bioactivation and detoxification between groups correlated with differences in the oxidation of NNK but not of NNAL. If the basis for these differences could be determined, identification of high and low categories for bioactivation and detoxification may be useful for predicting susceptibility of individuals to NNK-induced carcinogenesis. Results from this study are the first to suggest a role for CYP2A13 in NNAL formation. Although results do not support a role for either CYP2A13 or CYP2A6 as a major contributor to NNK bioactivation or detoxification in all individuals, results from subgroups of individuals suggest that CYP2A13 contributes to NNK metabolism, but this contribution varies between individuals.

Acknowledgements

The authors wish to thank Ms. Carole Fargo for administrative assistance.

References

Bedard LL, Smith GBJ, Reid K, Petsikas D, and Massey TE (2002) Investigation of the Role of Lipoxygenase in Bioactivation of 4-(Methylnitrosamino)-1-(3-pyridyl)-1-butanone (NNK) in Human Lung. *Chem.Res.Toxicol.* **15**:1267-1273.

Breyer-Pfaff U, Martin HJ, Ernst M, and Maser E (2004) Enantioselectivity of carbonyl reduction of 4-methylnitrosamino-1-(3-pyridyl)-1-butanone by tissue fractions from human and rat and by enzymes isolated from human liver. *Drug Metab Dispos.* **32**:915-922.

Day KC, Plopper CG, and Fanucchi MV (2006) Age-specific pulmonary cytochrome P-450 3A1 expression in postnatal and adult rats. *Am.J.Physiol Lung Cell Mol.Physiol* **291**:L75-L83.

Devereux TR, Belinsky SA, Maronpot RR, White CM, Hegi ME, Patel AC, Foley JF, Greenwell A, and Anderson MW (1993) Comparison of pulmonary O^6-methylguanine DNA adduct levels and Ki-ras activation in lung tumors from resistant and susceptible mouse strains. *Mol.Carcinog.* **8**:177-185.

Donnelly PJ, Stewart RK, Ali SL, Conlan AA, Reid KR, Petsikas D, and Massey TE (1996) Biotransformation of aflatoxin B_1 in human lung. *Carcinogenesis* **17**:2487-2494.

Fernandez-Salguero P and Gonzalez FJ (1995) The CYP2A gene subfamily: species differences, regulation, catalytic activities and role in chemical carcinogenesis. *Pharmacogenetics* **5**:S123-S128.

Fukami T, Nakajima M, Sakai H, Katoh M, and Yokoi T (2007) CYP2A13 metabolizes the substrates of human CYP1A2, phenacetin, and theophylline. *Drug Meta Dispos.* **35**:335-339.

Hecht SS (1998) Biochemistry, biology, and carcinogenicity of tobacco-specific *N*-nitrosamines. *Chem.Res.Toxicol.* **11**:559-603.

Hecht SS (1999) DNA adduct formation from tobacco-specific N-nitrosamines. *Mutat.Res.* **424**:127-142.

Hecht SS (2003) Tobacco carcinogens, their biomarkers and tobacco-induced cancer. *Nat.Rev.Cancer* **3**:733-744.

Hoffmann D, Rivenson A, and Hecht SS (1996) The biological significance of tobacco-specific N-nitrosamines: smoking and adenocarcinoma of the lung. *Crit Rev.Toxicol.* **26**:199-211.

Jalas JR, Ding X, and Murphy SE (2003) Comparative metabolism of the tobacco-specific nitrosamines 4-(methylnitrosamino)-1-(3-pyridyl)-1-butanone and 4-(methylnitrosamino)-1-(3-pyridyl)-1-butanol by rat cytochrome P450 2A3 and human cytochrome P450 2A13. *Drug Metab Dispos.* **31**:1199-1202.

Lowry OH, Rosebrough NJ, Farr AL, and Randall RJ (1951) Protein measurement with the folin phenol reagent. *J.Biol.Chem.* **193**:265-275.

Maser E, Stinner B, and Atalla A (2000) Carbonyl reduction of 4-(methylnitrosamino)-1-(3-pyridyl)-1-butanone (NNK) by cytosolic enzymes in human liver and lung. *Cancer Lett.* **148**:135-144.

McLemore TL, Adelberg S, Liu MC, McMahon NA, Yu SJ, Hubbard WC, Czerwinski M, Wood TG, Storeng R, Lubet RA, and et a (1990) Expression of cyp1a1 gene in patients with lung cancer: evidence for cigarette smoke-induced gene expression in normal lung tissue and for altered gene regulation in primary pulmonary carcinomas. *J.Natl.Cancer Inst.* **82**:1333-1339.

Messina ES, Tyndale RF, and Sellers EM (1997) A major role for CYP2A6 in nicotine C-oxidation by human liver microsomes. *J.Pharmacol.Exp.Ther.* **282**:1608-1614.

Miyamoto M, Umetsu Y, Dosaka-Akita H, Sawamura Y, Yokota J, Kunitoh H, Nemoto N, Sato K, Ariyoshi N, and Kamataki T (1999) CYP2A6 gene deletion reduces susceptibility to lung cancer. *Biochem.Biophys.Res.Commun.* **261**:658-660.

Patten CJ, Smith TJ, Murphy SE, Wang M-H, Lee J, Tynes RE, Koch P, and Yang CS (1996) Kinetic analysis of the activation of 4-(methylnitrosamino)-1-(3-pyridyl)-1-butanone by heterologously expressed human P450 enzymes and the effect of P450-specific chemical inhibitors on this activation in human liver microsomes. *Arch.Biochem.Biophys.* **333**:127-138.

Raunio H, Rautio A, Gullsten H, and Pelkonen O (2001) Polymorphisms of CYP2A6 and its practical consequences. *Br.J Clin.Pharmacol.* **52**:357-363.

Smith GBJ, Bend JR, Bedard LL, Reid KR, Petsikas D, and Massey TE (2003) Biotransformation of 4-(methylnitrosamino)-1-(3-pyridyl)-1-butanone (NNK) in peripheral human lung microsomes. *Drug Metab Dispos.* **31**:1134-1141.

Smith GBJ, Castonguay A, Donnelly PJ, Reid KR, Petsikas D, and Massey TE (1999) Biotransformation of the tobacco-specific carcinogen 4-(methylnitrosamino)-1-(3-pyridyl)-1-butanone (NNK) in freshly isolated human lung cells. *Carcinogenesis* **20**:1809-1818.

Smith TJ, Guo Z, Gonzalez FJ, Guengerich FP, Stoner GD, and Yang CS (1992) Metabolism of 4-(methylnitrosamino)-1-(3-pyridyl)-1-butanone in human lung and liver microsomes and cytochromes p-450 expressed in hepatoma cells. *Cancer Res.* **52**:1757-1763.

Smith TJ, Guo Z, Guengerich FP, and Yang CS (1996) Metabolism of 4-(methylnitrosamino)-1-(3-pyridyl)-1-butanone (NNK) by human cytochrome P450 1A2 and its inhibition by phenethyl isothiocyanate. *Carcinogenesis* **17**:809-813.

Smith TJ, Stoner GD, and Yang CS (1995) Activation of 4-(methylnitrosamino)-1-(3-pyridyl)-1-butanone (NNK) in human lung microsomes by cytochromes p450, lipoxygenase, and hydroperoxides. *Cancer Res.* **55**:5566-5573.

Su T, Bao Z, Zhang QY, Smith TJ, Hong JY, and Ding X (2000) Human cytochrome P450 CYP2A13: predominant expression in the respiratory tract and its high efficiency metabolic activation of a tobacco-specific carcinogen, 4-(methylnitrosamino)-1-(3-pyridyl)-1- butanone. *Cancer Res.* **60**:5074-5079.

Thun MJ, Lally CA, Flannery JT, Calle EE, Flanders WD, and Heath CW, Jr. (1997) Cigarette smoking and changes in the histopathology of lung cancer. *J Natl Cancer Inst* **89**:1580-1586.

von Weymarn LB, Brown KM, and Murphy SE (2006) Inactivation of CYP2A6 and CYP2A13 during nicotine metabolism. *J.Pharmacol.Exp.Ther.* **316**:295-303.

von Weymarn LB, Zhang QY, Ding X, and Hollenberg PF (2005) Effects of 8-methoxypsoralen on cytochrome P450 2A13. *Carcinogenesis* **26**:621-629.

Wang H, Tan W, Hao B, Miao X, Zhou G, He F, and Lin D (2003) Substantial reduction in risk of lung adenocarcinoma associated with genetic polymorphism in CYP2A13, the most active cytochrome P450 for the metabolic activation of tobacco-specific carcinogen NNK. *Cancer Res.* **63**:8057-8061.

Wei C, Caccavale KJ, Kenhoe JJ, Thomas PE, and Iba MM (2001) CYP1A2 is expressed along with CYP1A1 in human lung. *Cancer Lett.* **171**:113-120.

Wong HL, Zhang X, Zhang QY, Gu J, Ding X, Hecht SS, and Murphy SE (2005) Metabolic activation of the tobacco carcinogen 4-(methylnitrosamino)-(3-pyridyl)-1-butanone by cytochrome P450 2A13 in human fetal nasal microsomes. *Chem.Res.Toxicol.* **18**:913-918.

Yamazaki H, Inui Y, Yun CH, Guengerich FP, and Shimada T (1992) Cytochrome p450 2e1 and 2a6 enzymes as major catalysts for metabolic activation of n-nitrosodialkylamines and tobacco- related nitrosamines in human liver microsomes. *Carcinogenesis* **13**:1789-1794.

Zhang X, Su T, Zhang QY, Gu J, Caggana M, Li H, and Ding X (2002) Genetic polymorphisms of the human CYP2A13 gene: identification of single-nucleotide polymorphisms and functional characterization of an Arg257Cys variant. *J.Pharmacol.Exp.Ther.* **302**:416-423.

Zhu LR, Thomas PE, Lu G, Reuhl KR, Yang GY, Wang LD, Wang SL, Yang CS, He XY, and Hong JY (2006) CYP2A13 in human respiratory tissues and lung cancers: an immunohistochemical study with a new peptide-specific antibody. *Drug Metab Dispos.* **34**:1672-1676.

Footnotes

This work was supported by Canadian Institutes of Health Research (CIHR) grant no. MT10382.

Reprint requests:
Dr. Thomas E. Massey
Professor and Head
Department of Pharmacology and Toxicology
Queen's University
Kingston, ON K7L 3N6
Canada
E-mail. masseyt@queensu.ca

Legends for Figures

Figure 1. Metabolism of NNK. Metabolites I and II are detoxification products produced by pyridine *N*-oxidation; metabolites III to VI are endpoint products of α-hydroxylation and are indicative of the formation of unstable reactive metabolites which methylate or pyridyloxobutylate DNA*.

Figure 2. Correlation between the relative amount of CYP2A13 mRNA in human lung and the degree of NNK: **(a)** total α-hydroxylation (sum of four α-hydroxylation endpoint metabolites); **(b)** total *N*-oxidation (sum of two pyridine-*N*-oxidation metabolites); and **(c)** NNAL formation for each individual (n=27, Pearson's correlation). Levels of mRNA were determined by quantitative real-time RT-PCR and assessed using the comparative C_T method of relative quantitation, and are reported as values relative to patient 4JM.

Figure 3. Correlation between the relative amount of CYP2A6 mRNA in human lung as determined by quantitative real-time RT-PCR and the degree of NNK: **(a)** total α-hydroxylation (sum of four α-hydroxylation endpoint metabolites); **(b)** total *N*-oxidation (sum of two pyridine-*N*-oxidation metabolites); and **(c)** NNAL formation for each individual (n=23, Pearson's correlation). Levels of mRNA were determined by quantitative real-time RT-PCR as described for Figure 2.

Figure 4. Correlation between CYP2A enzyme activity as measured by the formation of 7-hydroxycourmarin from coumarin and the degree of NNK: **(a)** total α-hydroxylation (sum of four α-hydroxylation endpoint metabolites); **(b)** total *N*-oxidation (sum of two pyridine-*N*-oxidation metabolites) for each individual; and **(c)** NNAL formation (n=27, Pearson's correlation).

Figure 5. Correlation between CYP2A enzyme activity as measured by coumarin 7-hydroxylation and levels of **(a)** CYP2A13 mRNA and **(b)** CYP2A6 mRNA among individuals (n=26 and n=22, respectively, Pearson's correlation). Levels of mRNA were determined by quantitative real-time RT-PCR as described for Figure 2.

DMD Fast Forward. Published on August 23, 2007 as DOI: 10.1124/dmd.107.017343
This article has not been copyedited and formatted. The final version may differ from this version.

Table 1. Patient Demographics

Patient Code[a]	Age	Sex	Smoking History	Diagnosis Leading to Surgery	Drug Tx 1 Month Prior/Possible Occupational Exposure to Carcinogens
1IM	66	M	Current, 40 pckyrs	Squamous cell carcinoma	diltiazem HCL, salbutamol, budesonide, ranitidine, ASA
2LM	41	F	Current, 20 pckyrs	Adenocarcinoma	sotalol HCL, cilazapril, estrogen, omeprazole Mg
1LM	61	F	Current, 60 pckyrs	Adenocarcinoma	formoteral, budesonide, nizatidine
6JM	46	M	Current, 31 pckyrs	Squamous cell carcinoma	bupropion, codeine syrup
1KM	58	M	Current, 46 pckyrs	Adenocarcinoma	chlorodiazepoxide HCL, NSAID, carbamazapine, chlorodiazapam, flotatenine, lamotrigine
4JM	55	M	Current, 40-60 pckyrs	Non-small cell carcinoma	ASA, 3 glasses wine/day
2JM	60	F	Current, 40 pckyrs	Adenocarcinoma	conjugated estrogens, oxybutynin chloride, medroxyprogesterone, acetaminophen
5KM	68	M	Current, 55 pckyrs	Squamous cell carcinoma	acetaminophen, meloxicam
6KM	77	M	Former, 50 pckyrs	Squamous Carcinoma	metformin, ramipril, atenolol
4KM	69	M	Former, 35 pckyrs	Adenocarcinoma	atenolol, spironlactone/ Silica exposure
3KM	71	F	Former, 35 pckyrs	Adenocarcinoma, non-small cell carcinoma	pantoprazole, lexothyroxine sodium, clonidine, amitriptyline, lorazepam, lovastatin, salbutamol
8KM	55	F	Former, 15 pckyrs	Adenocarcinoma	conjugated estrogens, paroxetine HCL, hydrochlorothiazide, verapamil, montelukast sodium, fluticasone proprionate, naratriptan, ASA
7KM	56	F	Former, 28 pckyrs	Non-small cell carcinoma	sertraline, conjugated estrogens, ranitidine, meloxicam
1JM	55	F	Current, N/A	Adenocarcinoma	terbutaline sulfate, salbutamol, ipratropium bromide, steroids, glyburide, metformin, cisapride monohydrate, lansoprazole, fluoxitine HCL, budesonide, trazodone
3LM	61	M	Current, 20-30 pckyrs	Squamous Cell Carcinoma	Exposure to insulation
9KM	71	M	Former, 50 pckyrs	Non-small cell adenocarcinoma	None
5LM	73	F	Former, 4 pckyrs	Non-small cell adenocarcinoma	Amitriptyline
8JM	42	F	Current, 24 pckyrs	Adenocarcinoma	
7JM	57	F	Former, 40 pckyrs	Adenocarcinoma	Teacher
9JM	58	M	Current, 69 pckyrs	Adenocarcinoma	chlorodiazepoxide HCL, carbamazapine, chlorodiazapam, NSAID, ASA, flotatenine, lamotrigine
3JM	45	M	Current, 49.5 pckyrs	Adenocarcinoma	diazepam, fluvoxamine, warfarin
6LM	78	M	Current, 60 pckyrs	Non-small cell carcinoma/Adeno-squamous carcinoma	None
9LM	78	M	Former, N/A	Squamous Carcinoma	None
7LM	64	M	Former, 52.5 pckyrs	Non-small cell carcinoma	budesonide/formoterol fumarate, salbutamol, simvastatin, fluticasone
8LM	59	M	Current, N/A	Squamous cell carcinoma	ASA, pravastatin, glyceryl trinitrate
1MM	54	F	N/A, 39 pckyrs	Adenocarcinoma	None

2MM	65	M	Current, 40 pckyrs	Adenocarcinoma	alcohol, omeprazole Mg, ramipril
3MM	72	F	Former, 30 pckyrs	Adenocarcinoma	nifedipine, telmisartan, venlafaxine, atorvastatin, ASA
5JM	69	M	Former, 48 pckyrs	Squamous cell carcinoma	diazepam, ranitidine
6HM	68	F	Former, 40 pckyrs	Adenocarcinoma	levo thyroxine, oxazepam, multivitamin(17)

Abbreviations: M, Male; F, Female; pckyrs, Pack years (number of packs of cigarettes smoked per day times the number of years); N/A, information not available.
[a] Microsomes assigned codes for patient confidentiality

Table 2. Production of the four α-hydroxylation endpoint metabolites among high and low bioactivation groups.

	% Metabolite formation/mg protein/min					
	HA	Diol	HA + Diol	KAC	KAL	KAC + KAL
High bioactivation group	6.08 ± 4.45 *[a]	16.3 ± 43.3	22.4 ± 43.5†	350 ± 109 *	157 ± 123 *	192 ± 164*
Low bioactivation group	1.39 ± 2.23	1.39 ± 2.23	2.78 ± 3.15†	56 ± 54.2	6.11 ± 19.2	62.1 ± 57.5

[a] Data are presented as the mean ± SD metabolite formation values for each of the four metabolites in each group x 10^{-4}.
* Significantly different from low bioactivation group, Student's *t* test with Welch's correction.
† Total NNAL-derived metabolites (hydroxy acid plus diol) are significantly different from total NNK-derived metabolites (keto acid plus keto alcohol) in both bioactivation groups, Student's *t* test with Welch's correction.
Abbreviations: HA, hydroxy acid; KAC, keto acid; KAL, keto alcohol.

Table 3. Correlation analysis between the extent of CYP2A immunoinhibition and the degree of NNK biotransformation, levels of CYP2A mRNA, and 7-hydroxycoumarin formation.

		% Change in total α-hydroxylation[a]		% Change in total *N*-oxidation		% Change in NNAL formation	
Total α-hydroxylation (n=29)		r=0.234[b]	*P*=0.222[b]				
	High bioactivation group	r=0.285	*P*=0.268				
	Low bioactivation group	r=0.313	*P*=0.322				
Total *N*-oxidation (n=29)				r=0.177	*P*=0.360		
	High detoxification group			r=0.218	*P*=0.573		
	Low detoxification group			r=0.156	*P*=0.512		
NNAL formation (n=29)						r=-0.0362	*P*=0.852
CYP2A13 mRNA (n=28)		r=0.0861	*P*=0.633	r=0.0586	*P*=0.767	r=0.112	*P*=0.569
CYP2A6 mRNA (n=24)		r=-0.338	*P*=0.107	r=0.0815	*P*=0.705	r=-0.0234	*P*=0.960
7-Hydroxycoumarin formation (n=27)		r=0.0200	*P*=0.920	r=0.125	*P*=0.533	r=0.00856	*P*=0.966

[a] CYP2A6/13 immunoinhibition was determined by the % change in NNK metabolism in the presence of a CYP2A6/13 inhibitory antibody. Immunoinhibition experiments were performed independently of other experiments that assessed NNK metabolism, mRNA expression and coumarin 7-hydroxylation.
[b] Correlation coefficients (r) and *P* values determined using Pearson's correlation analysis.

Figure 1

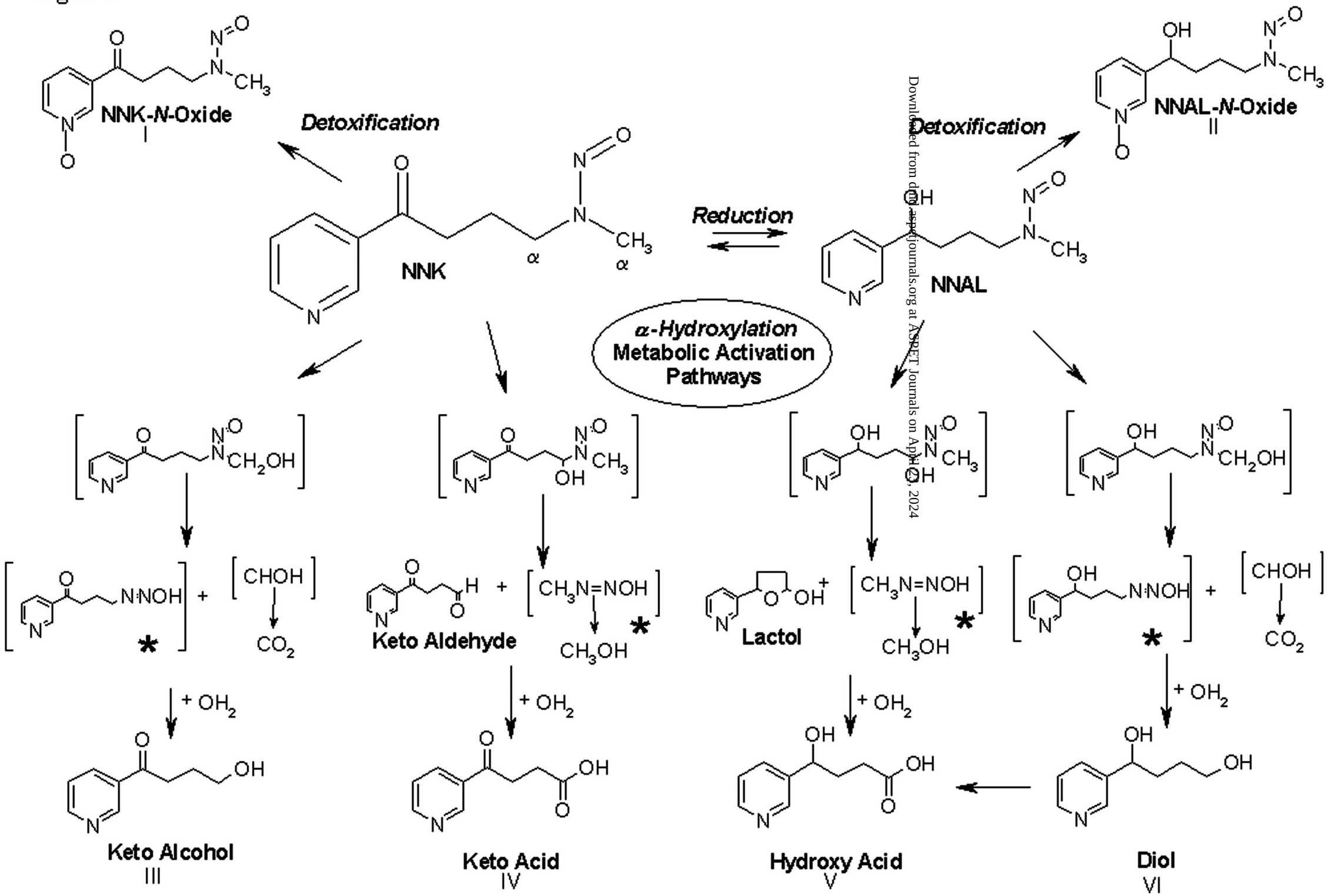

Figure 2

(a)

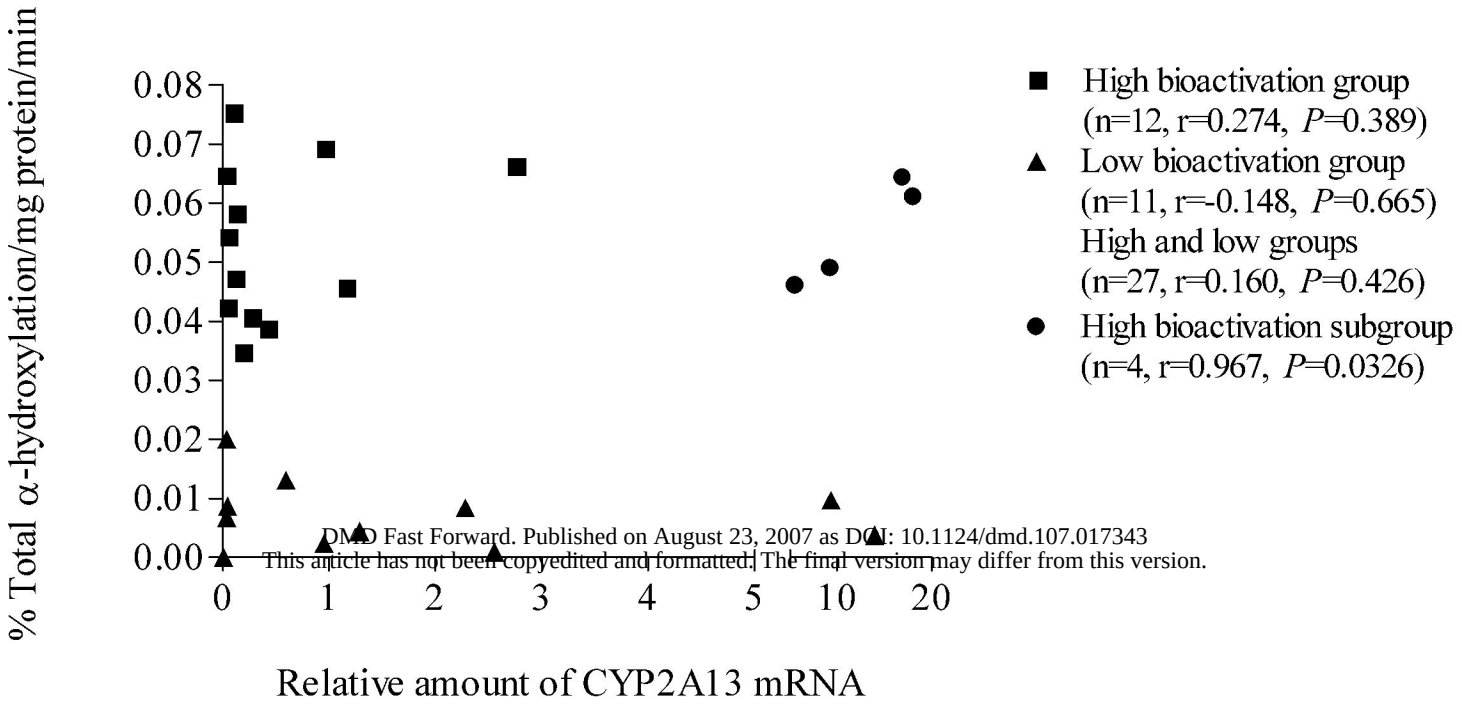

(b)

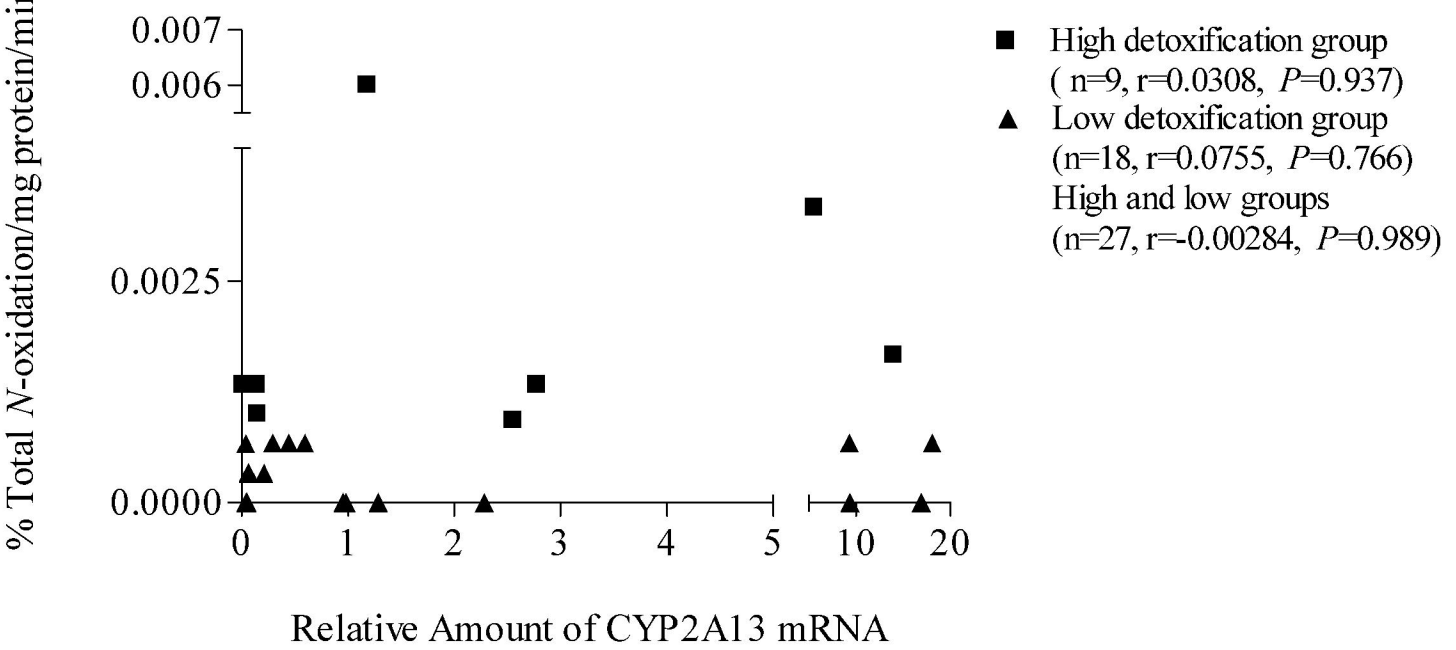

(c)

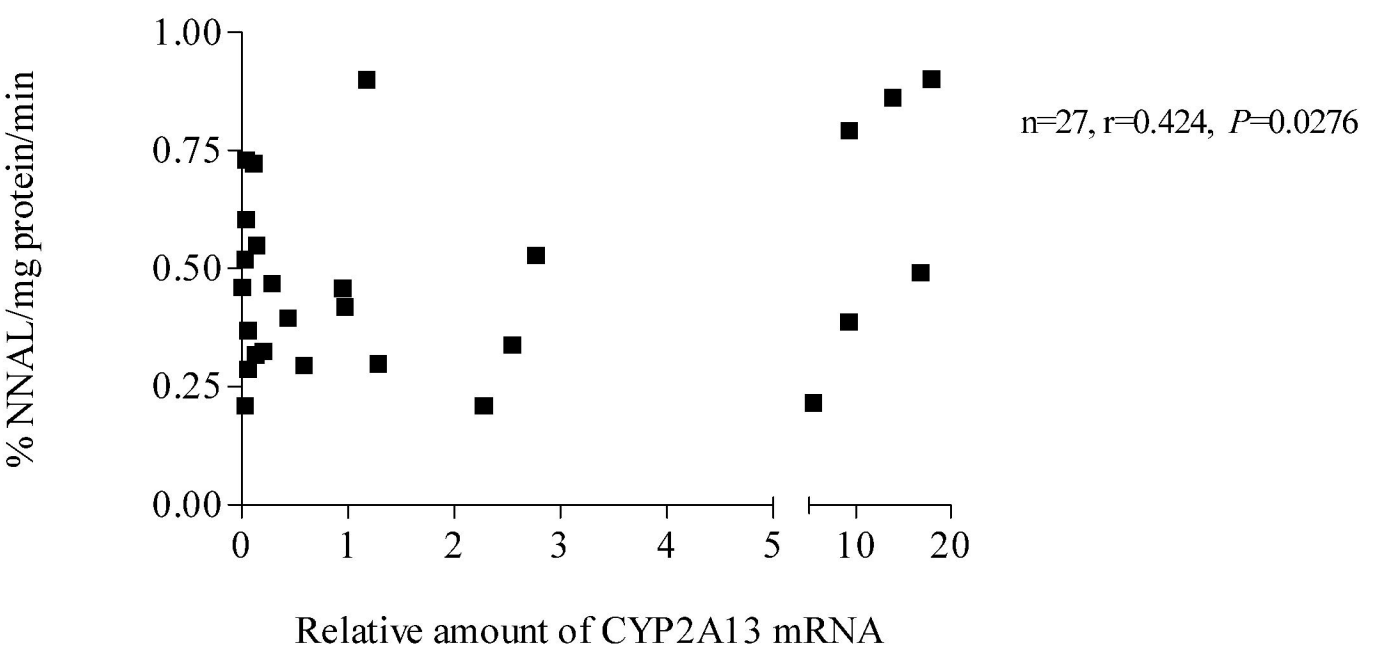

Figure 3

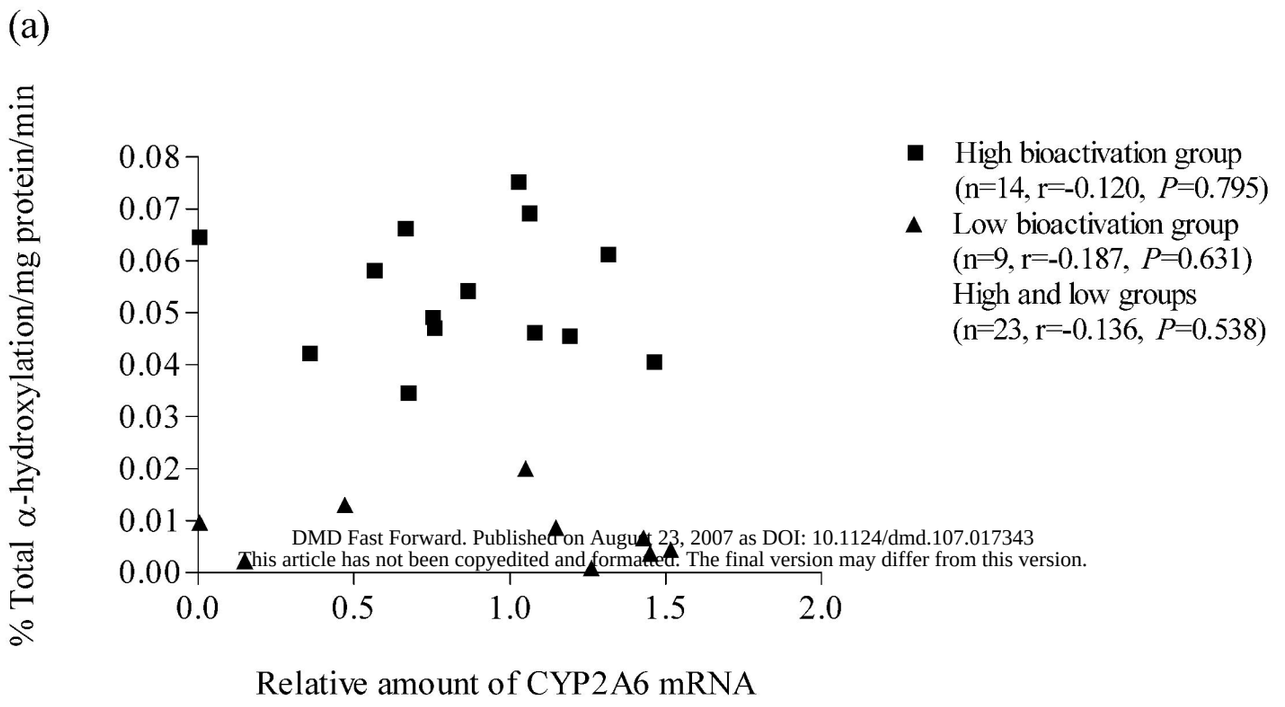

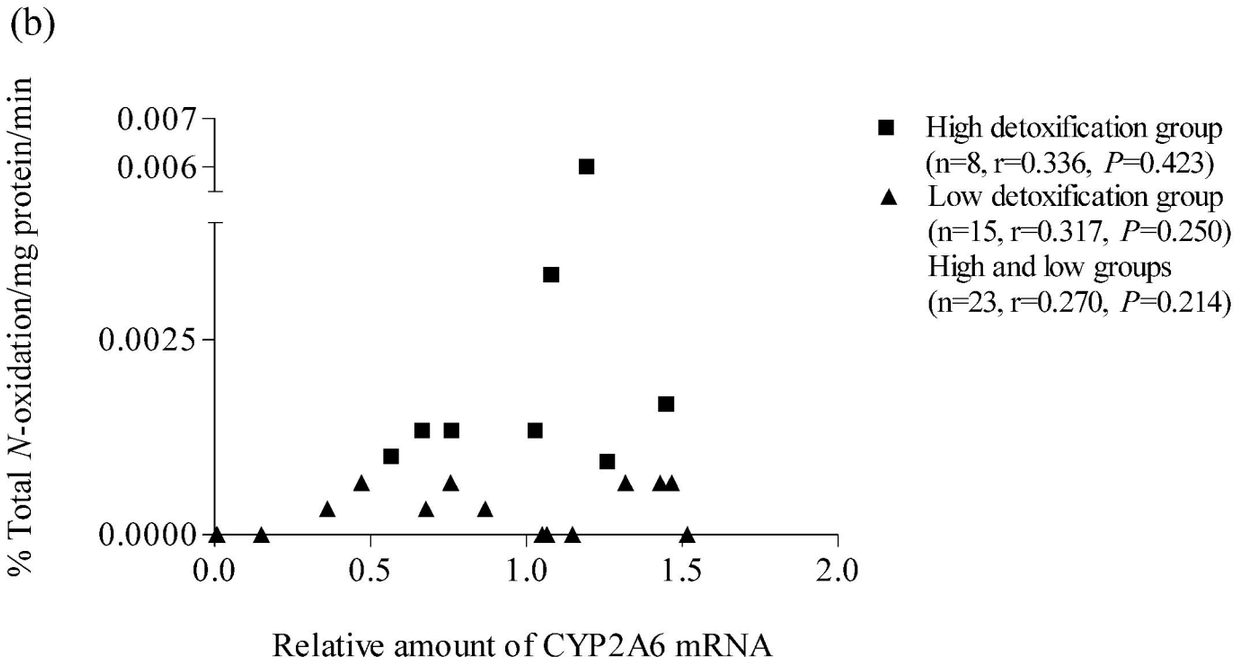

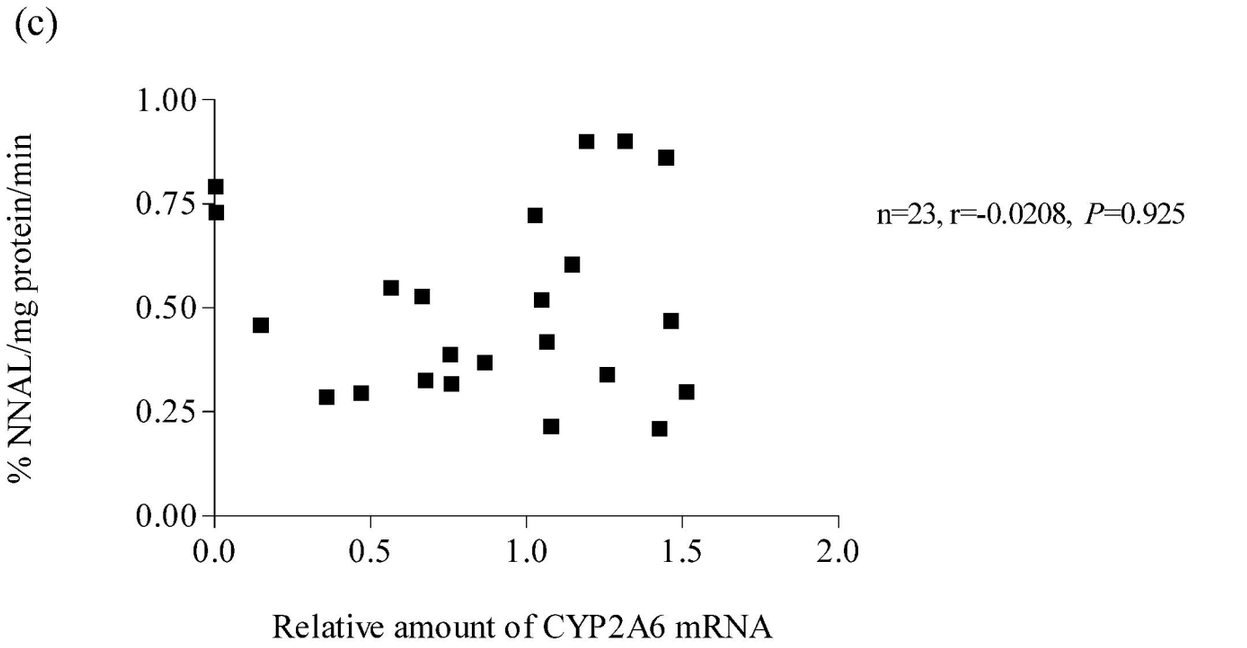

Figure 4

(a)

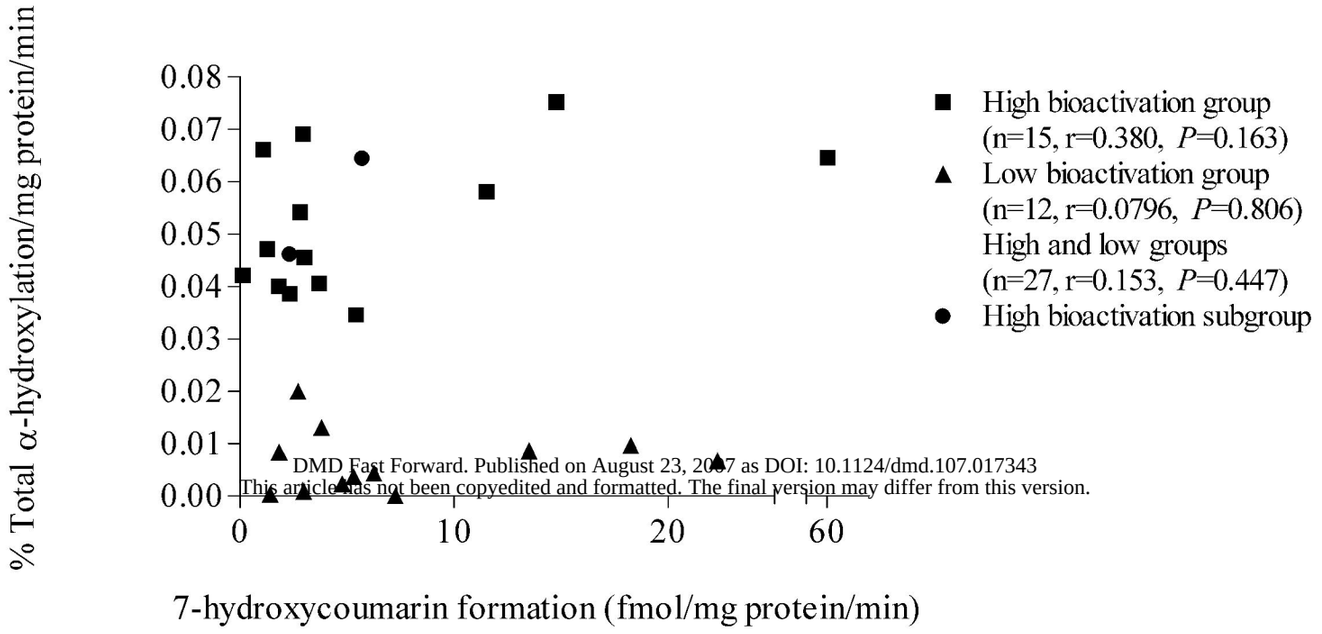

(b)

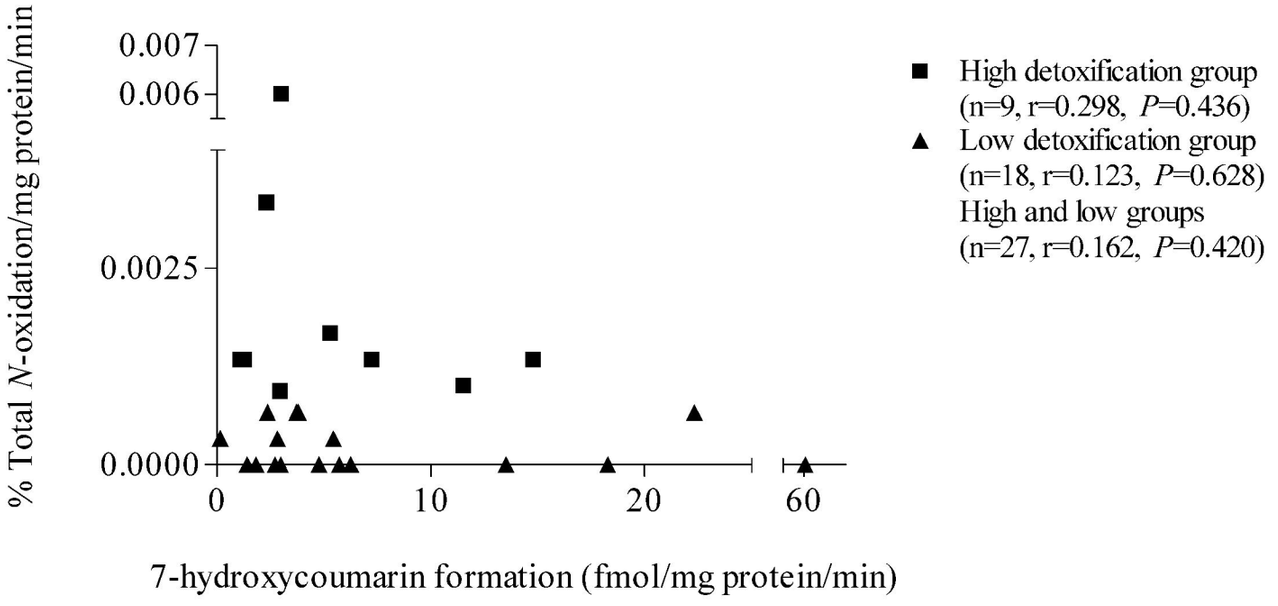

(c)

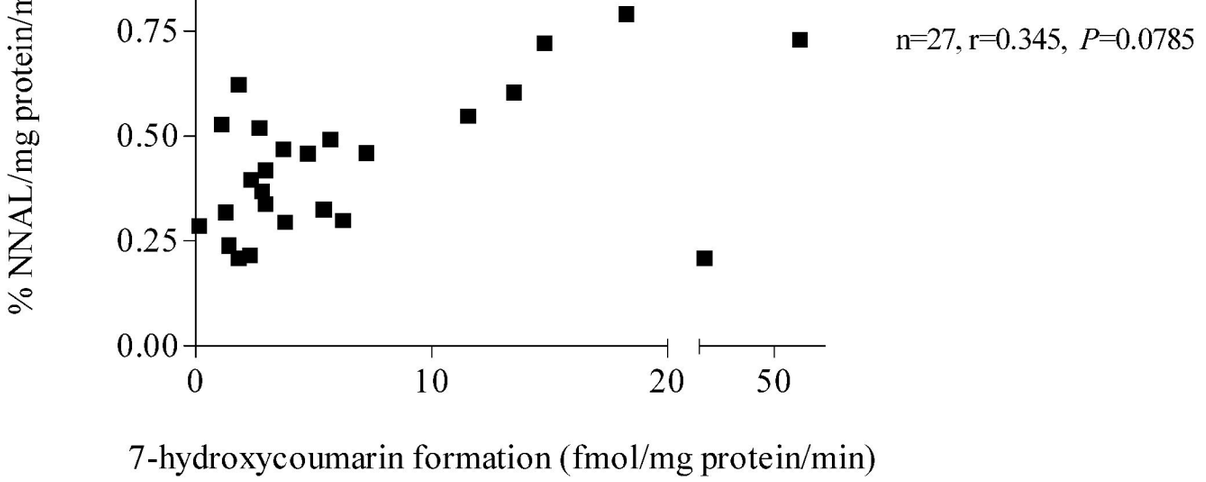

Figure 5